
EFDA–JET–PR(04)54

I. Voitsekhovitch, X. Garbet, D. C. McDonald, K.-D. Zastrow, M. Adams, Yu. Baranov,
P. Belo, L. Bertalot, R. Budny, S. Conroy, J. G. Cordey, L. Garzotti, P. Mantica,
D. McCune, J. Ongena, V. Parail, S. Popovichev, D. Stork, A. D. Whiteford
and JET EFDA Contributors

Density Dependence of Trace Tritium Transport in H-mode JET Plasma

Density Dependence of Trace Tritium Transport in H-mode JET Plasma

I. Voitsekhovitch¹, X. Garbet², D. C. McDonald¹, K.-D. Zastrow¹, M. Adams¹, Yu. Baranov¹, P. Belo³, L. Bertalot⁴, R. Budny⁵, S. Conroy⁶, J. G. Cordey¹, L. Garzotti⁷, P. Mantica⁸, D. McCune⁵, J. Ongena⁹, V. Parail¹, S. Popovichev¹, D. Stork¹, A. D. Whiteford¹⁰ and JET EFDA Contributors*

¹EURATOM/UKAEA Fusion Association, Culham Science Centre, Abingdon, OXON, OX14 3DB UK

²Association EURATOM/CEA Cadarache, F-13108, St Paul lez Durance, France

³EURATOM/IST Fusion Association, Centro de Fusão Nuclear, Lisbon Portugal

⁴Associazione EURATOM/ENEA sulla Fusione, Frascati, Italy

⁵PPPL, Princeton University, Princeton, NJ, 08543, USA

⁶Deptartment of neutron Research, Uppsala University. EURATOM-VR Association, Sweden

⁷Consorzio RFX, Associazione EURATOM/ENEA sulla Fusione, Padova, Italy

⁸Istituto di Fisica del Plasma, EURATOM-ENEA-CNR Association, Milan, Italy

⁹LPP-ERM KMS Association EURATOM/Belgian State, Brussels, Belgium

¹⁰Dept. of Physics, University of Strathclyde, Glasgow, UK

* See annex of J. Pamela et al, "Overview of Recent JET Results and Future Perspectives", Fusion Energy 2002 (Proc. 19th IAEA Fusion Energy Conference, Lyon (2002)).

“This document is intended for publication in the open literature. It is made available on the understanding that it may not be further circulated and extracts or references may not be published prior to publication of the original when applicable, or without the consent of the Publications Officer, EFDA, Culham Science Centre, Abingdon, Oxon, OX14 3DB, UK.”

“Enquiries about Copyright and reproduction should be addressed to the Publications Officer, EFDA, Culham Science Centre, Abingdon, Oxon, OX14 3DB, UK.”

ABSTRACT

Tritium transport in Edge Localized Mode (ELMy) high confinement (H-mode) plasmas is analysed here as a function of density for discharges from the recent trace tritium experimental campaign performed on Joint European Torus. In this campaign small amounts of tritium have been puffed or injected (with neutral beam injectors) into deuterium plasmas [8]. Information about the tritium has been obtained from the evolution of the profiles of neutron emission simulated via the TRANSP [16] and SANCO [17] codes. A strong inverse correlation of tritium transport with plasma density is found in this analysis. The low tritium transport at high density is close to neoclassical values while the transport becomes strongly anomalous in low density plasmas. The thermal transport does not exhibit such a strong density dependence, leading to a varying ratio of thermal to tritium transport in these pulses. An interpretation of the density effects on the trace tritium transport, partially based on the test particle simulations in plasmas with stochastic magnetic field, is proposed. A simple model for the tritium diffusion coefficient and convective velocity, which includes the modification of the neoclassical particle diffusion in presence of electromagnetic turbulence [14] completed with an empirical density dependence, is developed. This model has positive β -dependence in agreement with the results of the similarity experiments performed for trace tritium transport.

I. INTRODUCTION

Particle transport is a key issue for experimental tokamak scenarios where the density control is important (e.g. the high density operation with dual deuterium and impurity feedback control on Joint European Torus (JET) [1] or the long pulse operation on Tore Supra [2]). The peculiarity of particle transport, as compared to thermal energy transport, is the comparable conductive and convective fluxes, whose separate values (i.e., diffusion and convective velocity) cannot be derived from the steady-state particle balance equation. The conventional approach to particle transport includes perturbative experiments (modulated gas puff, pellet injection) and the analysis of naturally occurring plasma perturbations (low to high confinement (L-H) transition, sawtooth crashes, etc.) where the particle diffusion coefficient and convective velocity can be separated.

Modulation experiments with the deuterium (D) gas puff in deuterium plasmas have been performed in a number of machines [3-9]. The most important result of these experiments is the existence of a strong anomalous pinch at the plasma edge in the ohmic and low confinement (L-mode) regime, and the scaling of particle transport with plasma parameters. It was found that the particle diffusion increases with the edge safety factor q (or alternatively reduces with poloidal magnetic field and plasma current) [3,4,6], reduces with plasma density [3,5,6] and increases with electron temperature [4]. The particle pinch has a scaling similar to that of diffusion coefficient [3, 4] suggesting similar physical mechanism driving the conductive and convective anomalous flux.

The experiments with tritium gas puff into deuterium plasmas performed at JET [7-9] showed a similar scaling of tritium transport with plasma parameters. The strong inverse correlation of the tritium diffusion coefficient with plasma density was found in the high confinement (H-mode)

plasmas [10] and confirmed for other scenarios (hybrid scenario, discharges with internal transport barrier (ITB)) [8]. The strong dependence of tritium diffusion on the edge safety factor was also observed [8]. In terms of dimensionless scaling, the gyro-Bohm scaling of trace tritium in the core and Bohm-like scaling at the edge have been found in the H-mode JET plasmas [7]. The tritium diffusion and convective velocity have similar scalings with the plasma parameters [8] to those found for deuterium transport [4]. The tritium diffusion reduces in the region of the transport barrier produced by reversed shear [8] similar to results with enhanced reversed shear in Tokamak Fusion Test Reactor (TFTR) [11].

The inverse correlation of the tritium and deuterium diffusion coefficients with plasma density is one of the common observations of the experiments mentioned above. This paper is focused on the detailed transport analysis of the trace tritium discharges from the recent experimental campaign on JET where the density effect on trace tritium transport has also been observed [10]. The objective of this analysis in addition to the experimental illustration of the correlation between the tritium transport and plasma density, is the comparison of the density effect on the energy and tritium transport and the identification of the physical mechanisms which could explain the observed density effect. The predictive modelling of the trace tritium discharges with theory-based models is used for the identification of the physical mechanisms. First, the Multi-Mode Model (MMM) [12] based on the electrostatic turbulence, which computes the full matrix of transport coefficients and separates the diffusive and convective fluxes has been tested. It was found that the MMM model fails to explain the density effect on tritium transport, over-predicting the diffusion at high density by an order of magnitude and under-predicting it at low density. However, the thermal ion and electron transport is well reproduced with the MMM model in the same discharges. Thus, the predictive modelling shows that in high density plasmas where the trace tritium transport is nearly neoclassical, the thermal transport is strongly anomalous and in agreement with the drift mode driven transport in its quasi-linear approximation. The transition of the tritium transport from neoclassical to anomalous is investigated by predictive modelling assuming the electromagnetic turbulence-driven trace particle transport and in particular taking into account the modification of the neoclassical transport in stochastic magnetic fields [13, 14]. A simple model for tritium transport coefficients based on the test particle simulations [14] which also includes an empirical density dependence matching the tritium transport at high and medium density is developed, and tested over a broader density range. This model has positive β -dependence, confirming the results of the similarity experiments performed for trace tritium transport [15].

This paper is organised as follows. First, the experimental scenarios with tritium gas puff, and the diagnostics used to follow the tritium evolution will be described (Section 2). The tritium transport coefficients in plasmas with different density obtained in the interpretative analysis performed with TRANSP code [16] and with the combination of TRANSP code and SANCO code [17] will be presented in Section 3. The predictive modelling of the trace tritium discharges is shown in Section 4, the results are summarized in the final section

2. EXPERIMENTAL SCENARIO WITH TRITIUM GAS PUFF

Tritium gas puff experiments analysed here have been performed in deuterium H-mode plasmas with Edge Localised Modes (ELMs) heated by deuterium Neutral Beam Injection (NBI). The parameters of three discharges with strongly different density selected for the more detailed analysis with the TRANSP code are given in Table 1. The NBI power in these discharges varied from 2.3 to 13.6MW. The deuterium gas puff is increased from zero at low power to 4.4×10^{22} electrons per second at high power. As a result, the plasma density varies from $n_l = 2.4 \times 10^{19} \text{ m}^{-3}$ to $9.5 \times 10^{19} \text{ m}^{-3}$ (here, n_l is the central line averaged density obtained with the Thomson scattering diagnostics). The magnetic field and plasma current are slightly different in these discharges ($B_{tor} = 1.9 - 2.25\text{T}$, $I_{pl} = 2 - 2.5\text{MA}$ (Table 1)), but the safety factor profiles are similar. Pulse No: 61132 and 61097 are performed at low triangularity $d_l = 0.18 - 0.19$ and $d_u = 0.22 - 0.26$ (here d_l and d_u are low and upper triangularity correspondingly) and the high density discharge has high triangularity ($d_l = 0.37$, $d_u = 0.44$). The difference in the electron and ion temperature in these discharges is less than 25%. Thus, the parameter displaying the most strong variation is the plasma density, which varies by factor 4. The scenarios of these discharges and the electron density profiles during the Tritium (T_2) gas puff are shown in Fig.1.

The T_2 gas is puffed for 80ms from the low field side during the stationary phase of the discharge. The amount of puffed tritium is about 6mg, which provides less than 5% of the tritium concentration. Since the direct measurement of the tritium density is not available, the trace tritium is detected by measuring the 14MeV neutrons produced in the deuterium-tritium (DT) reaction. The neutron measurements are performed along the 10 horizontal and 9 vertical chords using the neutron profile monitor with 10ms time resolution [18]. In addition, the total DT neutron yield is measured by two different detectors and compared with the neutron yield integrated over the chords. The chords of measurements cover the plasma region from the plasma centre to 0.82 of minor radius (the lines of sight of the neutron monitor are shown in Fig.2).

The neutron yield of the DT reaction depends not only on the tritium content, but also on the ion temperature T_i and deuterium concentration. The bulk deuterium density n_D is estimated from the measurements of the electron density n_e and effective charge of plasma Z_{eff} while the fast deuterium density is calculated by TRANSP. The ion temperature and Z_{eff} profile in trace tritium discharges have been measured using the Charge-eXchange (CX) spectroscopy with 50ms time resolution. Up to 50 channels of the Thomson scattering diagnostics, with 250ms time resolution, are used for the measurements of electron density and temperature (T_e) profiles. Since the low density Pulse No: 61132 analysed here exhibits strong sawtooth activity, the Electron Cyclotron Emission (ECE) measurements of electron temperature with 0.4ms time resolution have been used for this discharge to resolve the T_e evolution during the sawtooth crashes. The plasma profiles obtained with these diagnostics are consistent with other measurements such as the loop voltage, total DD neutron yield before and after the tritium puff and diamagnetic energy where the fast particle content calculated with TRANSP is added to the thermal energy content estimated with the measured plasma profiles.

3. INTERPRETATIVE ANALYSIS OF TRACE TRITIUM TRANSPORT

The conventional approach to the analysis of perturbative experiments includes three steps: (i) the choice of the parameterisation for the radial profile of particle transport coefficients, (ii) the estimation of particle sources and the solution of the particle balance equation with parameterised transport coefficients and (iii) the adjustment of the parameters determining the shape of these coefficients to match the available experimental data [3 - 8]. Usually a simple piece-wise parameterisation for the particle diffusion and convective velocity is applied, which includes the constant values in certain plasma regions with a linear interpolation between these regions providing the continuous radial dependence [3-8]. Such parameterisation is limited in many studies by two or three regions with constant value for diffusion and convective velocity where these coefficients can be considered as an averaged transport. In the TRANSP simulations of trace tritium discharges we assume a radially constant or piece-wise diffusion coefficient, but the shape of the convective velocity is not parameterised and is calculated at each radial grid point as described below. Thus, the poor parameterisation of the diffusion coefficients is improved by the local estimation of the particle convection. The tritium convective velocity is estimated from the sum of the continuity equations for deuterium and tritium which includes the NBI and wall recycling source of deuterium, the gas puff and recycling tritium source and the imposed deuterium and tritium diffusion. This equation is solved self-consistently with the quasi-neutrality constraint. Since the tritium is present in the negligible amount, the quasi-neutrality condition determines mainly the deuterium density taking into account experimental value of Z_{eff} and electron density while the continuity equation summed over all the species determines the convective velocity. Then, the tritium density evolution is simulated with its continuity equation using prescribed diffusion coefficient and calculated convective velocity.

The estimation of the tritium source is an important issue of this analysis. The tritium ions in these discharges are produced through the ionization of puffed tritium neutrals and recycled neutrals. The puffed and recycled neutrals exhibit primary ionization and multiple charge exchange with thermal and fast deuterium penetrating deeper in plasma and being ionised there. These primary and secondary atomic processes are simulated using the FRANTIC code [19] built into TRANSP. The influx of puffed tritium neutrals through the Last Closed Flux Surface (LCFS) is estimated by taking into account the total amount of injected tritium and the time evolution of the tritium emission at 656.04nm (T_α) measured along the line-of-sight looking at the valve. The temporal shape of the tritium influx is estimated from the shape of the T_α emission re-normalised to provide the penetration of all injected tritium through the LCFS. In principle, all tritium neutrals puffed into the Scrape-Off-Layer (SOL) do not necessarily penetrate through the LCFS, they fill the SOL and divertor region and may stay there. Thus, the tritium influx through the separatrix is a free parameter of these simulations. However, the transport coefficients inside $r/a < 0.8$ (here $r = \Phi^{0.5}$, $a = \Phi_{boundary}^{0.5}$, Φ is the toroidal flux) depend on the tritium influx into this region (i.e. the region inside $r/a = 0.8$) rather than the tritium influx through the separatrix. The influx into $r/a = 0.8$ as well as the tritium transport coefficients inside $r/a < 0.8$ are adjusted to match the neutron data. The influx adjustments

is performed in TRANSP by choosing the transport at $r/a > 0.8$ to provide the same tritium flux into the region $r/a \leq 0.8$ even if the tritium flux through the separatrix is different. Namely, the too large tritium influx through the LCFS is reduced by the large outward convection at the periphery in TRANSP simulations while the small influx is amplified by the inward convection. Since there are no neutron measurements at the plasma periphery the transport in this region and the influx through the LCFS cannot be experimentally validated.

The wall recycling is also important for the estimation of tritium transport coefficients and confinement time. To reduce the uncertainty in the choice of transport and recycling each discharge with the tritium gas puff has been accompanied by a discharge with the same parameters, but with a short (up to 150ms) and low power (1MW) application of tritium NBI fuelling replacing the gas puff. In the discharges with NBI fuelling the recycling source is less important as compared to the central tritium source. The paired discharges with tritium beam and gas puff have been analysed together and the tritium diffusion coefficients and recycling have been adjusted to match the evolution of puffed tritium as well as the decay of the thermalised tritium in the partner discharges with beam fuelling. The recycled tritium influx in the discharges with the gas puff is prescribed as a fraction of the total (deuterium and tritium) flux and this fraction is used as an adjustable parameter. For the discharges analysed here the tritium recycling flux is about 3 – 4% of the total recycling flux increasing to 7% during the sawteeth in Pulse No: 61132. Finally, it should be mentioned that the boundary value of the tritium density is chosen to be small enough that it does not affect the results of simulations.

As mentioned above the input parameters of the TRANSP simulations (tritium diffusion coefficient and recycled fraction) are adjusted to match the 14MeV neutron emission profile and the total DT neutron yield. The approach used here does not give the estimation of the error bars on the transport coefficients. Instead, the accuracy in the choice of transport coefficients is characterised by the agreement between measured and calculated neutron emission for all chords of measurements. The

quantitative parameter used for comparison is defined as $\chi^2 = \frac{1}{20N} \sum_{i=1}^{20} \sum_{j=1}^N (Y_{ij,exp} - Y_{ij,sim})^2 / \sigma_i^2$ (here $Y_{j,exp}$ is the experimentally measured neutron emission along the 19 chords (see Fig.2) and the total neutron yield, $Y_{j,sim}$ is their simulated values, σ_i is the standard deviation of measured signal and N is the number of time points). The typical values of normalised χ^2 obtained by adjusting the diffusion coefficient and tritium recycling in TRANSP simulations are in the range 2.44 – 3.72. These values of χ^2 are not very accurate taking into account that a good value of χ^2 is approximately 1. However, they characterise a reasonable agreement with the neutron data (fig.3). The simulated neutron emission is shown in fig.3 for 6 horizontal channels located in the bottom of the machine (channels 4-9, Fig.2). Similar agreement is obtained for other channels. The discrepancy with the neutron data for the Pulse Nos:61097 and 61138 can be partially explained by weak sawtooth activity which is not included in TRANSP simulations of these discharges. The low density discharge displays strong sawtooth oscillations which are taken into account in the simulations assuming the Kadomtsev reconnection model [20] implemented in TRANSP code [21].

The tritium transport coefficients for three selected discharges are shown in Fig.4. A reasonable fit of the neutron emission is obtained with the simplest assumption of flat diffusion coefficient D_T for the low and medium density discharges (Fig.4). However, the assumption of radially constant D_T does not lead to a satisfactory agreement with the neutron measurements for the high density plasma. That is why the piece-wise diffusion coefficient is used for this discharge and its shape is adjusted to match the neutron emission (Fig.4, dashed curve). As one can see, the core tritium diffusion coefficient D_T in these discharges exhibits the inverse correlation with plasma density. At high density, the diffusion coefficient approaches its neoclassical value estimated with NCLASS [22] while at low density the tritium transport is anomalous. The large diffusion losses in low density H-mode plasma are partially compensated by a strong inward convective velocity V_T while the tritium convective velocity is much lower at high density. The small diffusion and convective velocity leads to the low tritium penetration in high density plasma, but the tritium penetrates rapidly when the plasma density is low (Fig.5).

Another mechanism providing the fast non-diffusive penetration of tritium in the plasma centre is sawtooth activity. As mentioned above, the sawtooth oscillations are clearly observed in the ECE measurements of electron temperature in these discharges. The effect of the sawtooth crashes on the mixing of various plasma species has been shown in Ref. 10, and the detailed analysis of this effect at different plasma density will be presented elsewhere. Here, the effect of the sawtooth crashes on the evolution of puffed tritium ions is briefly described since it is important for the low density discharge.

The sawtooth oscillations are simulated for Pulse No: 61132 using the Kadomtsev model with full reconnection of the current density profile within the inversion radius ($r_{inv}/a \sim 0.5$). This model maintains the core safety factor profile close to one. The electron and ion temperature exhibiting the sawtooth crashes have been taken from the measurements while the fast particle and tritium mixing was simulated by TRANSP. The time evolution of the central tritium density and the density profile during the sawtooth crashes are shown in Fig.6. Interestingly, the sawteeth occurring during the rise phase, when the tritium density profile is hollow, accelerate the tritium penetration towards the plasma core while the fast deuterium particles are removed from the centre. The sawtooth crashes enhance the tritium removal from the core during the decay phase when the tritium density profile is peaked.

Tritium transport has been compared to thermal transport for the discharges of the density scan. The thermal effective diffusivity estimated with TRANSP taking into account the NBI heating, ohmic heating of electrons, energy losses due to the atomic processes (charge-exchange and ionization) and radiative losses does not display a clear correlation with the plasma density leading to the density dependent ratio χ_{eff}/D_T (Fig. 7). This result may have an impact on the modelling of International Thermonuclear Experimental Reactor (ITER) scenarios with different density where the assumption about the constant ratio of thermal to bulk particle (and helium) diffusion coefficient independent on the plasma density is made (see for example Ref. 23). If the transport mechanism of different plasma species (bulk ions and helium) is similar to the trace tritium transport the ratio of thermal to particle diffusion should vary with density in these scenarios, that would affect the estimated fusion performance.

The strong correlation between tritium transport and plasma density demonstrated in the analysis of three discharges with the TRANSP code has been found also using another analysis method [8, 24]. In this method, the neutron reactivity (i.e., the ratio of neutron emission to the tritium density) calculated by TRANSP has been used for post-processing the results from the fast predictive code SANCO which solves the tritium diffusion equation, calculates the neutron emission and re-adjusts the transport coefficients and recycling flux by minimising χ^2 -value [8, 24]. This method gives a closer fit of the neutron data with smaller χ^2 and allows to estimate the error bars for the transport coefficients as a statistical errors, however the equilibrium model used in SANCO is less sophisticated than the model used in TRANSP. The tritium diffusion coefficients from this method for 9 NBI heated Hmode discharges performed at different magnetic field, plasma current and heating power [8] are shown in Fig.8. These coefficients were assumed constant in the plasma core ($r/a < 0.4$) and they are plotted in Fig.8 as a function of the plasma density averaged over the same region. Similarly strong dependence of tritium diffusion on plasma density has been observed also in the outer part of plasma however the data points are more scattered than in Fig. 8 because of the strong dependence of DT on the other parameters like for example, the safety factor q [8]. In spite of the number of the differences between TRANSP and SANCO models (different equilibrium, metrics and parametrisation of the transport coefficients) leading to some variations in the values of diffusion coefficient both techniques clearly demonstrate the reduction of the diffusion coefficient with plasma density. At high density, the tritium diffusion coefficients are close to the neoclassical value (the upper and low limits of neoclassical transport in the considered density range determines the shaded region in Fig. 8). The scattering in the core diffusion coefficients for the discharges performed at the same density is due to the difference in other plasma parameters [8].

4 PREDICTIVE MODELLING OF TRACE TRITIUM DISCHARGES

In this Section, the physical mechanisms underlying the correlation between the tritium transport and plasma density are investigated through predictive modelling with different theory-based transport models using the ASTRA code [25]. The modelling of the tritium density profile has been performed with the tritium sources and current density profile calculated in TRANSP. The electron and ion temperature profiles are also taken from TRANSP, but they represent a fit to the experimental data. First, the analysis of the trace tritium discharges with the MMM model based on electrostatic turbulence will be described. Then, a new model which includes some parametric dependencies following from test particle simulations in stochastic magnetic field will be introduced and tested. The tritium density evolution obtained with these models will be compared with the density obtained in the interpretative TRANSP analysis (Section 3).

a) MMM model

As a first step the maximum linear growth rate of drift modes is calculated with the MMM model for the discharges from Table I to check the correlation between the turbulence growth rate and plasma density (Fig.9). This is done by using the experimental temperature and density profiles

including the tritium density found in Section 3. In high and medium density discharges (Fig.9(a)) the Ion Temperature Gradient (ITG) instability is the dominant in the gradient region while the Trapped Electron Mode (TEM) is larger at the edge. The ITG growth rate reduces with plasma density being comparable with the TEM growth rate in low density plasma. The profile modifications during the sawtooth crashes sometimes lead to the slight increase of the TEM which becomes the dominant instability (such case is shown in Fig.9b). Thus, the stability analysis shows that the increase of the plasma density does not lead to the turbulence stabilisation which could explain the suppression of the anomalous tritium transport at high density.

As a next step, the thermal energy balance has been simulated using the full matrix of transport coefficients and taking the experimental density profile and heat sources and sinks (NBI and ohmic heating, electron-ion exchange, energy losses due to atomic processes and electron radiative losses) calculated in TRANSP. The MMM model used here includes the drift mode driven transport (ITG and TEM) and resistive ballooning transport. This model predicts reasonably well the electron and ion temperature profiles in low density plasmas (Fig.10, top) and slightly overestimates the anomalous transport at high density (Fig.10, bottom). The modelling of the ion temperature in the discharge 61138 with the neoclassical transport only, over-predicts the core temperature by 37% indicating that the anomalous transport is really important in this discharge. In high density plasma, the anomalous thermal transport is comparable to the neoclassical transport, while the thermal losses are mainly driven by the drift modes and the neoclassical thermal flux is negligible in the Pulse No: 61132.

The modelling of the trace tritium with the MMM model is not so straightforward. The present version of the MMM model includes two plasma species, main hydrogen species and impurity. The main hydrogen species can include the deuterium-tritium mixture with averaged concentration. However, such approach is not suitable for the modelling of the trace tritium since the averaging procedure gives a nearly pure deuterium plasma. For this reason, the tritium is treated as an “impurity” in our simulations while the carbon impurity density measured by the CX diagnostics is taken into account in the quasi-neutrality condition and estimation of Z_{eff} . The continuity equation for tritium includes also the neoclassical flux which is rather large due to the DT collisions.

The tritium evolution simulated with the MMM model is shown in Fig.11. The MMM model over-estimates the diffusion coefficient, predicting a too rapid accumulation and decay of particles in high and medium density discharges. In contrast, the convective velocity and core diffusion are too low in the Pulse No: 61132 resulting in a slower rise and decay of the core tritium density.

b) Model based on tritium diffusion in stochastic electromagnetic field

The MMM model shows that the electrostatic turbulence is strongly unstable even in the case of high densities where the tritium analysis indicates that the transport is near neoclassical. Indeed, the maximum linear growth rate is larger at high density (Fig.9) and the anomalous thermal transport is not negligible in the Pulse No: 61138. A few questions arise from these observations: why the tritium diffusion is unaffected or weakly affected by the turbulence at high density where the thermal

transport is essentially anomalous; what is the physical mechanism of the anomalous trace tritium transport; and how can the density dependence of tritium transport be explained.

Regarding the last question, the inverse dependence of the tritium transport on plasma density may be expressed as an inverse dependence on the collisionality. Such inverse dependence of particle diffusion on collisionality is opposite to one expected from the collisional transport where the diffusion coefficient increases with collisionality. It can hardly be explained by the collisionality dependence of the anomalous transport missing in the present version of the MMM model. Firstly, the collisionality affects the TEM turbulence while the estimation with the MMM model shows that the ITG is the dominant instability in the considered density range, being comparable with the TEM only at low density. Secondly, the density peaking factor $n_e(r/a=0)/\langle n_e \rangle$ (here n_e is the electron density and $\langle \rangle$ stands for volume averaging) is slightly higher in the medium density Pulse No: 61097 (~ 1.3) than in the low density Pulse No: 61132 (~ 1.25) breaking the trend with collisionality expected from the TEM driven particle flux.

On the other hand, the inverse density dependence is an important feature of the transport based on the electromagnetic turbulence. Indeed, the diffusion coefficient due to particle collisions can be roughly estimated as $D \sim L^2 n \chi_{oll}$ (here L is the characteristic radial excursion of particles and ν_{coll} is the collisional frequency). The relevant small radial excursions of particles in a homogeneous toroidal magnetic field is the Larmor radius, whilst this increases to the banana orbit width in the poloidal magnetic field for particles trapped in the inhomogeneous tokamak fields. A larger diffusion scale appears with the stochastisation of magnetic field where the closed particle trajectories have the width proportional to the characteristic scale of the fluctuating Hamiltonian [26]. In this regime, the collisional diffusion coefficient is replaced by an expression of the type $D \sim L_f^2 \nu_L$ where L_f is the characteristic fluctuation length and ν_L is the statistically-averaged frequency of encountering an excursion of size L_f . Since the particle excursions are caused by the magnetic field fluctuations their characteristic scale is determined by the skin depth, $L_f \sim L_{skin} \sim c/\omega_{pe} \sim 1/n_e^{0.5}$. So that in plateau regime the diffusion coefficient will have an inverse density dependence.

The transport model based on the electromagnetic turbulence has been developed previously for the electron thermal [27] and electron particle [28, 29] transport. The transition from electrostatic to electromagnetic anomalous thermal flux occurs at high poloidal beta β_p , i. e, the electromagnetic transport is expected to become dominant with the density increase at fixed magnetic field and temperature. This model has been successfully tested on the Tore Supra discharges showing the dominant electromagnetic transport in the core plasma heated by fast waves [27] while the thermal and particle transport in the low density Lower Hybrid Enhanced Performance (LHEP) discharges is well described by the MMM model based on the electrostatic turbulence [30].

The simulations of the stochastic test particle transport in electromagnetic turbulence [14, 28] give the general understanding of the basic physical mechanisms and some parametric dependencies of the transport rather than analytical expression suitable for the modelling of the experimental scenarios. However, such analytical expression can be developed on the basis of the test particle

simulations. It will be necessary to include some fitting coefficients and even additional parametric dependencies which must be determined from the modelling of experimental discharges. In what follows, such a model for trace tritium transport is developed using the discharges representing the density scan. First, the model proposed in Ref.14 is completed with the empirical density dependence matching the tritium transport in the high and medium density discharges. Then, this model is tested on the discharge with low density. This semi-empirical transport model is expressed also as a function of the dimensionless parameters β , ρ^* and ν^* (these parameters are defined in Ref.15) for the comparison with the results of the similarity experiments performed for the trace tritium [15].

Following the above discussion, the trace tritium radial excursion should be estimated as $\max\{\rho_T, L_{skin}\}$ for passing particles (where ρ_T is the tritium Larmor radius) and $\max\{\Delta_{ban}, L_{skin}\}$ for trapped particles (where Δ_{ban} is the width of tritium banana trajectory). The trapped particle losses dominate for the most of the plasma volume, and hence we focus on these. Then the diffusion coefficient can be estimated as $D_T \sim D_{neocl} \max\{1, (L_{skin} / \Delta_{ban})^2\} \sim D_{neocl} \max\{1, (c / (\omega_{pe} \Delta_{ban}))^2\}$ where ω_{pe} is the plasma frequency and c is the speed of light. However, this estimation is very approximate since it includes the low limit of the particle radial shift. The test particle simulations reveal the group of particles with very large trajectories (so called percolating trajectories) whose contribution to the diffusion coefficient is important [14]. Taking this into account we will look for the diffusion coefficient as a function of $\omega_{pe}^{-\alpha}$ where $\alpha > 2$ and will determine the α -value from the fit of tritium evolution in the Pulse No:61138 and 61097. Assuming the same mechanism for the diffusion and convection we will look for the similar expression for the convective velocity where the exponent in the ω_{pe} -multiplier will be also adjusted. As it is done in Section 4(a) the tritium evolution is simulated using the tritium sources and plasma equilibrium calculated by TRANSP and the experimental temperature and density profiles. As a result, the following model for the trace tritium diffusion coefficient and convective velocity is found:

$$\begin{aligned}
 D_T &= D_{T, ncl} \max\left\{1, 2(R/L_n)^{4/7}\right\} \max\left\{1, C_1 \left(\sqrt{(c_s/R)\omega_B} / \omega_{pe}\right)^{\alpha_D}\right\} \\
 V_T &= V_{T, ncl} \max\left\{1, 2(R/L_n)^{4/7}\right\} C_2 \left(\sqrt{(c_s/R)\omega_B} / \omega_{pe}\right)^{\alpha_V}
 \end{aligned} \tag{1}$$

Here, $D_{T, ncl}$ and $V_{T, ncl}$ are the neoclassical transport coefficients calculated with NCLASS, $C_1 = 5.79 \cdot 10^{23}$, $C_2 = 4.61 \cdot 10^{15}$, $\alpha_D = 7$, $\alpha_V = 4.5$, R is the major radius, $L_n = n_e / \nabla n_e$ is the characteristic density gradient length, c_s is the sound speed of tritium and ω_B is the electron gyro-frequency. The multiplier $(c_s/R) \omega_B$ is used for the normalisation of the ω_{pe} -dependent parameter controlling the deviation from the neoclassical transport. Following Ref.14 the density-dependent stochastic correction has the additional multiplier $(R/L_n)^{4/7}$, characterising the statistical distribution of long trajectories. The thresholds in the stochastic correction of the neoclassical transport are introduced in Eq.(1) to avoid the reduction of the transport coefficients below the neoclassical level when the density profile is flat.

The evolution of the tritium density at different radii (Fig.12) and the tritium density profile (Fig.13) obtained with the model of Eq.(1) for three discharges from Table 1 show a good agreement with the tritium density obtained from the fit of neutron data (Section 3). The small discrepancy with the interpretative results in the low density discharge can be explained by the sawtooth activity, which is not implemented in the modelling. As it was shown in Section 3 the sawtooth activity provides the fast non-diffusive tritium penetration in the plasma core and enhances the losses during the decay phase. Thus, the transport coefficients proposed here can be considered as a sawtooth-averaged transport. These coefficients (Fig.14) are in reasonable agreement with the values obtained in Section 3 (Fig.4). In high density plasma, the core tritium transport is close to the neoclassical (Fig.14(a) and 14(b)). The enhancement of the neoclassical transport in this discharge occurs due to the R/L_n multiplier in Eq.(1) indicating that only the particle moving along the very long trajectories contribute to the anomalous losses (the second multiplier is below the threshold). At low and medium density, both anomalous corrections, which increase the transport above neoclassical, become important.

The enhancement factors for neoclassical tritium diffusion and convective velocity (i.e. the ratio $D_T/D_{T,ncl}$ and $V_T/V_{T,ncl}$ correspondingly) described by Eq.(1) can be expressed in terms of dimensionless parameters as $(\beta v^*)^{-1.75}$ and $(\beta v^*)^{-1.25}$. The neoclassical transport itself does not depend on β , but the correction factor found in the predictive modelling of discharges with different density introduces the β -dependence in tritium transport. This dependence is favourable because the reduction of the diffusive tritium flux with the increase of β exceeds the reduction of convective flux. This conclusion is in the qualitative agreement with the similarity experiments performed during the trace tritium campaign which also confirm the favourable β effect on tritium transport [15].

SUMMARY AND DISCUSSION

The results of the interpretative analysis of trace tritium transport in the NBI heated ELMy H-mode plasmas on JET can be summarised as follows:

1. A strong inverse correlation of tritium transport with plasma density is found using two different analysis methods. The tritium diffusion is close to its neoclassical value at high density while it is strongly anomalous at low density;
2. The tritium convective velocity is close to the neoclassical one in high density plasma, but it becomes anomalous at low density;
3. The thermal effective diffusivity does not display such strong density dependence leading to a density dependence for the ratio χ_{eff}/D_T ,
4. The trace tritium is strongly affected by the sawtooth activity. The sawteeth redistribute the tritium differently during the rise and decay phase, enhancing its penetration in the core in the rise phase when the tritium profile is hollow and its removal in the decay phase when the profile is peaked.

Predictive modelling of the trace tritium evolution has been performed with the goal of understanding the density effect on the tritium transport. Firstly, the MMM model based on the electrostatic drift

mode turbulence has been tested. This model fails to predict the trace tritium transport, while it gives a satisfactory prediction of thermal transport in the same discharges. The stability analysis performed with this model shows that electrostatic turbulence is not reduced with the plasma density.

A hypothesis about the electromagnetic nature of the tritium transport based on the test particle behaviour in a stochastic magnetic field is proposed. This hypothesis could explain the inverse correlation of the tritium transport with density for the set of discharges representing the density scan. Another argument in favour of the electromagnetic nature of tritium transport is its inverse dependence on β found in the similarity experiments with tritium gas puff [15]. A situation similar to these JET discharges, i.e., a weak β -dependence of thermal transport indicating its electrostatic nature in discharges with favourable β -dependence of trace helium transport has also been observed on DIII-D [31]. This situation is puzzling from the point of view of turbulent theories and simulations predicting that generally the electromagnetic effects are weak.

Based on the assumption of the electromagnetic nature of particle transport a correction to the neoclassical trace tritium transport caused by the stochastic magnetic field has been developed and tested giving quite satisfactory agreement with the results of the interpretative analysis. The density dependence included in this model is stronger than the one following from a simple mixing length argument, indicating a possible non-linear diffusion mechanism at low density. It must be mentioned that the transport coefficients with the density dependence proposed here cannot be considered as a final complete transport model. A dependence of tritium transport on other plasma parameters such as q and ρ_{pol} has also been found [8]. The effects of these parameters have to be understood and implemented in the transport model. This is the subject of future work.

ACKNOWLEDGEMENTS

Drs. G. Pereverzev and A. Zolotukhin are warmly acknowledged for assistance in using the NCLASS implemented in ASTRA code. This work was performed under the European Fusion Development Agreement, and partly funded by EURATOM and the UK Engineering and Physical Sciences Research Council.

REFERENCES

- [1]. P. Dumortier, G. Bonheure, R. Felton, J. Harling, E. Joffrin, A. Messiaen, J. Ongena, P. Belo, L. Bertalot, I. Coffey, Y. Corre, K. Crombe, M.de Baar, A. Huber, D. Kalupin, A. Kreter, S. Jachmich, G. Maddison, P. Monier-Garbet, A. Murari, M.F.F. Nave, V. Parail, S. Popovichev, M.E. Puiatti, G. Telesca, M. Tokar, B. Unterberg, M. Valisa, I. Voitsekhovitch, M.von Hellermann and JET EFDA Contributors, Dual Feedback Controlled High Performance Ar Seeded ELMy H-mode Discharges in JET including Trace Tritium Experiments, Proceedings of the 31st European Conference on Controlled Fusion and Plasma *Physics*, London, UK, 2004, to be published
- [2]. T. Wijnants and G. Martin, *Nucl. Fusion*, **36**, 1201 (1996)
- [3]. K. W. Gentle, O. Gehre and K. Krieger, *Nucl. Fusion* **32**, 217 (1992)

- [4]. J. O'Rourke, C. Gowers, G.J. Kramer, P.D. Morgan, R. Simonini and A.C.C. Sips, *Plasma Phys. Contr. Fusion* **35**, 585 (1993)
- [5]. D.R. Baker, M.R. Wade, G.L. Jackson, R. Maingi, R.E. Stockdale, J.S. deGrassie, R.J. Groebner, C.B. Forest, G.D. Porter and DIII-D Team, *Nucl. Fusion* **38**, 485 (1998)
- [6]. J.P.T. Koponen, T. Geist, U. Stroth, S. Fiedler, H.-J. Hartfuss, O. Heinrich, H. Walter, ECH Group, W7-AS Team and O. Dumbrajs, *Nucl. Fusion* **40**, 365 (2000)
- [7]. K.-D. Zastrow and JET Team, *Nucl. Fusion* **39**, 1891 (1999)
- [8]. K.-D. Zastrow, J. M. Adams, Yu. Baranov, *et al*, *Plasma Phys. Contr. Fusion* **46**, B255 (2004)
- [9]. D. Stork, Yu. Baranov, P. Belo, *et al*, Overview of Transport, Fast Particle and Heating and Current Drive Physics using Tritium in JET plasmas, *Proceedings of 20th IAEA Fusion Energy Conference*, Vilamoura, Portugal, 2004, (International Atomic Energy Agency, Vienna, 2005), paper OV/4-1, to be published
- [10]. I. Voitsekhovitch, D.C. McDonald, K.-D. Zastrow, *et al*, Transport Analysis of Trace Tritium Experiments on JET using TRANSP Code and Comparison with Theory-Based Transport Models, *Proceedings of the 31st European Conference on Controlled Fusion and Plasma Physics*, London, UK, 2004, to be published
- [11]. P.C. Efthimion, S. von Goeler, W.A. Houlberg, *et al*, *Phys. Plasmas* **5**, 1832 (1998)
- [12]. G. Bateman, A.H. Kritz, J.E. Kinsey, A.J. Redd and J. Weiland, *Phys. Plasmas* **5**, 1793 (1998)
- [13]. P.N. Yushmanov, *JETP Letters* **52**, 217 (1990)
- [14]. A.I. Smolyakov and P. Yushmanov, *Nucl. Fusion* **33**, 383 (1993)
- [15]. D.C. McDonald, J.G. Cordey, K.-D. Zastrow, *et al*, Particle and Energy Transport in Dedicated ρ^* , β and v^* Scans in JET ELMy H-modes, *Proceedings of 20th IAEA Fusion Energy Conference*, Vilamoura, Portugal, 2004, (International Atomic Energy Agency, Vienna, 2005), paper EX/6-6, to be published
- [16]. R.J. Goldston, D.C. McCune, H.H. Towner, S.L. Davis, R.J. Hawryluk and G.L. Schmidt, *J. Comput. Phys.* **43**, 61 (1981)
- [17]. L. Lauro-Taroni, B. Alper, R. Giannella, K. Lawson, F. Marcus, M. Mattioli, P. Smeulders, M. Von Hellermann, *Proceedings of the 21st European Conference on Controlled Fusion and Plasma Physics*, Montpellier, France, 1994, vol. I, p.102
- [18]. S. Popovichev, L. Bertalot, M. Adams, *et al*, Performance of Neutron Measurements during Trace Tritium Experiments on JET, *Proceedings of the 31st European Conference on Controlled Fusion and Plasma Physics*, London, UK, 2004, to be published
- [19]. A.A. Korotkov and A.N. Zinov'ev, *Sov. Journal Plasma Phys.* **15**, 136 (1989)
- [20]. B.B. Kadomtsev, *Sov. Journal Plasma Phys.* **1**, 389 (1975)
- [21]. R. Budny, M.G. Bell, A.C. Janos, *et al*, *Nucl. Fusion* **35**, 1497 (1995)
- [22]. W.A. Houlberg, K.C. Shaing, S.P. Hirshman, M.C. Zarnstorff, *Phys. Plasmas*, **4**, 3230 (1997)
- [23]. A.R. Polevoi, M. Sugihara, H. Takenaga, A. Isayama, N. Oyama, A. Loarte, G. Saibene, and G.V. Pereverzev, *Nucl. Fusion* **43**, 1072 (2003)

- [24]. A. Whiteford, K.-D. Zastrow, M. Adams, *et al*, Quantitative Forward Modelling of Neutron Emission to Derive Transport Coefficients of Tritium in JET, including Error Propagation through to Transport Parameters, *Proceedings of the 31st European Conference on Controlled Fusion and Plasma Physics*, London, UK, 2004, to be published
- [25]. G.V. Pereverzev, F. X. Soldner, R. Bartiromo, F. Leuterer, and V. V. Parail, *Nucl. Fusion* **32**, 1023 (1992)
- [26]. M.B. Isichenko, J. Kalda, E.B. Tatarinova, O.V. Telkovskaya, and V.V. Yankov, *Sov. Phys. JETP* **69**, 517 (1989)
- [27]. W. Horton, P. Zhu, G.T. Hoang, T. Aniel, M. Ottoviani and X. Garbet, *Phys. Plasmas* **7**, 1494 (2000)
- [28]. D.E. Kim, D.-I. Choi, W. Horton, P.N. Yushmanov and V.V. Parail, *Phys. Fluids* **B2**, 547 (1990)
- [29]. V.V. Parail, P.N. Yushmanov, *JETP Letters* **42**, 343 (1985)
- [30]. I. Voitsekhovitch, G. Bateman, A.H. Kritz and A. Pankin, *Phys. Plasmas* **9**, 4241 (2002)
- [31]. C.C. Petty, T.C. Luce, D.C. McDonald, *et al*, *Phys. Plasmas* **11**, 2514 (2004)

Pulse No:	B_t , T	I_{pl} , MA	P_{NBI} , MW	Central line density, 10^{19} m^{-3}
61132	1.90	2.35	2.3	2.4
61097	1.65	2.00	7.6	5.0
61138	2.25	2.50	13.6	9.5

JG05.24-15c

Table I: Parameters of the NBI heated ELMy H-mode discharges with the tritium gas puff.

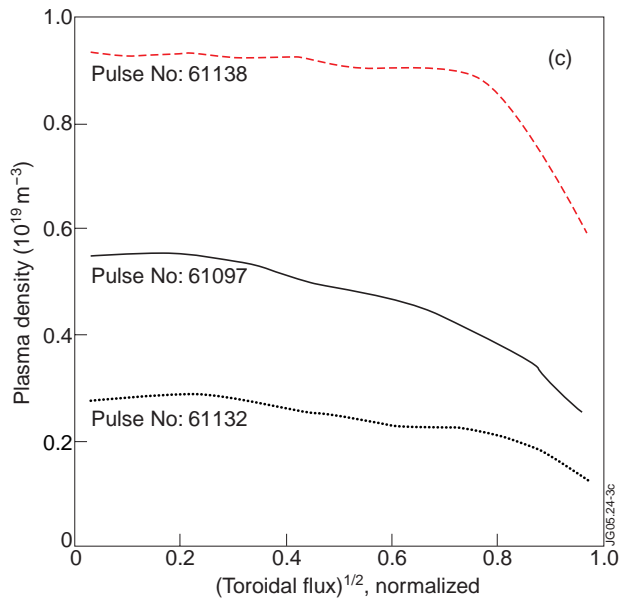
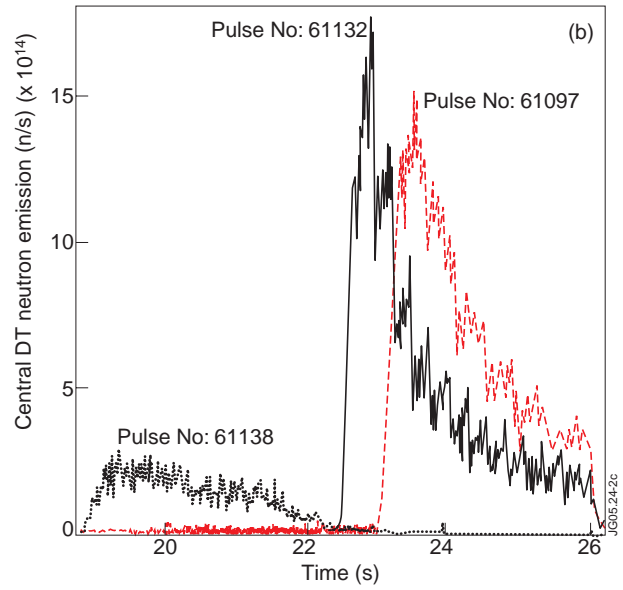
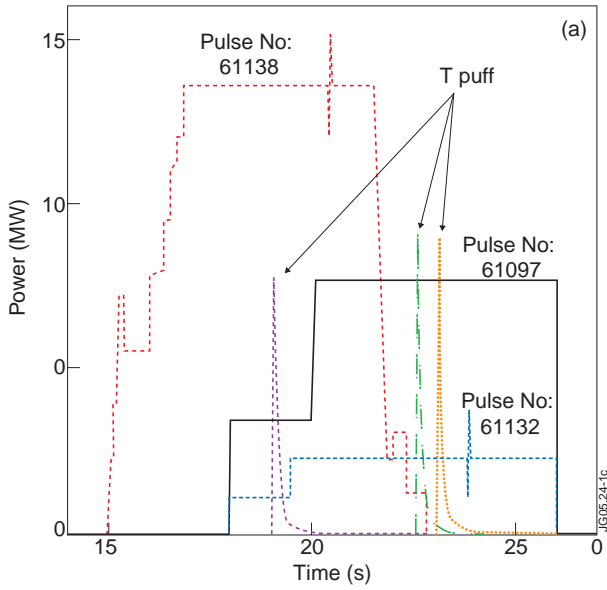


Figure 1: Scenarios of the pulses representing the density scan: NBI power and tritium puff (a), central DT neutron emission measured along the horizontal chord (b) and electron density profiles during the T_2 gas puff (c).

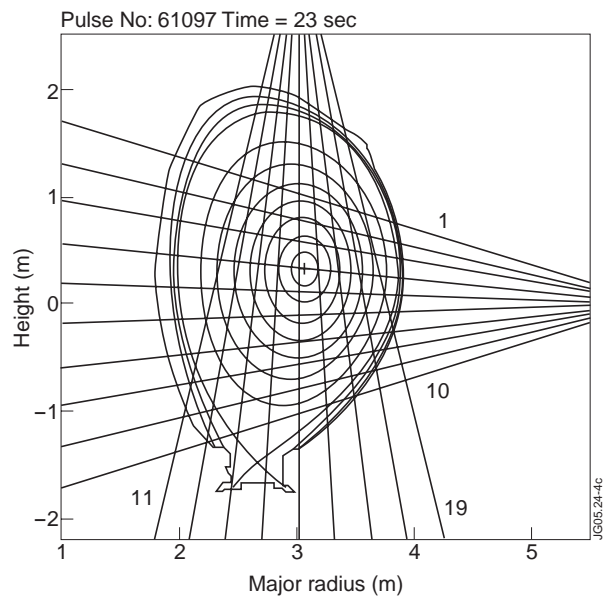


Figure 2: Lines of sight of the neutron profile monitor with the number for each line of sight.

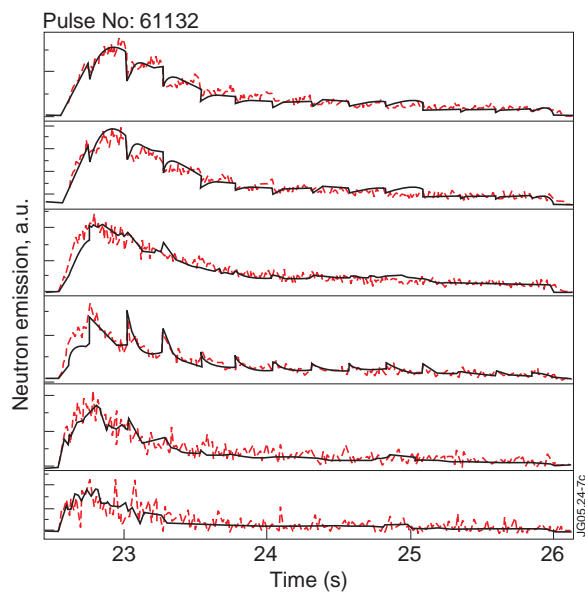
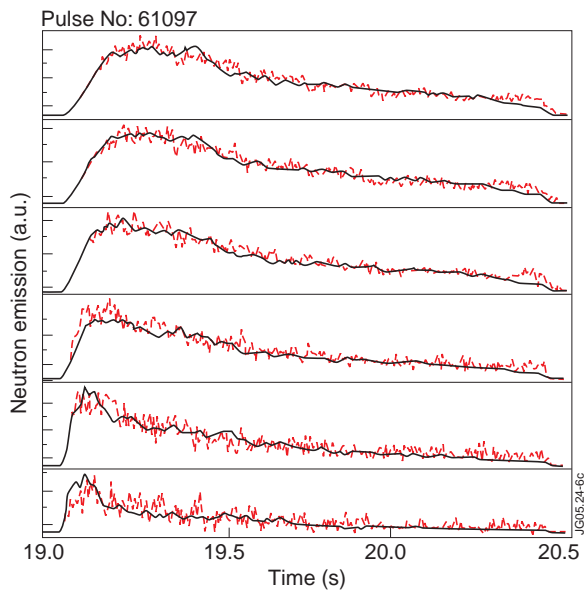
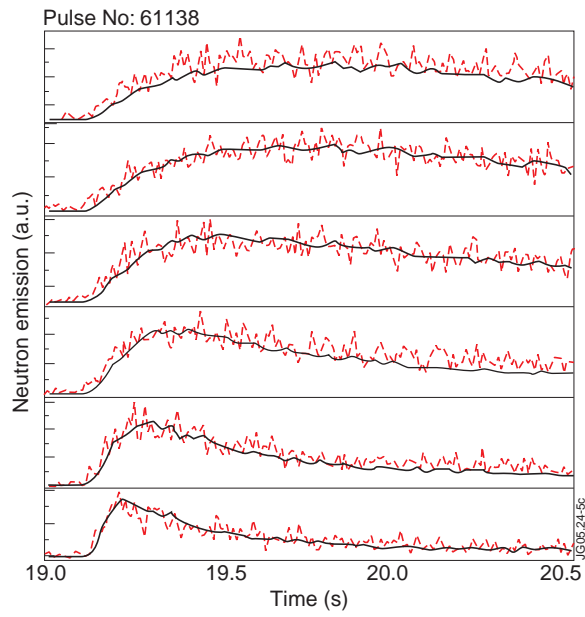


Figure 3: Neutron emission measured along the horizontal lines of sight of the neutron monitor n° 4-9 (thin curves) and calculated along the same lines of sight in TRANSP (bold curves) for the Pulse No: 61138 (top), 61097 (middle) and 61132 (bottom). $\chi^2 = 2.44$ for Pulse No: 61138, $\chi^2 = 2.53$ for 61097 and $\chi^2 = 3.72$ for 61132.

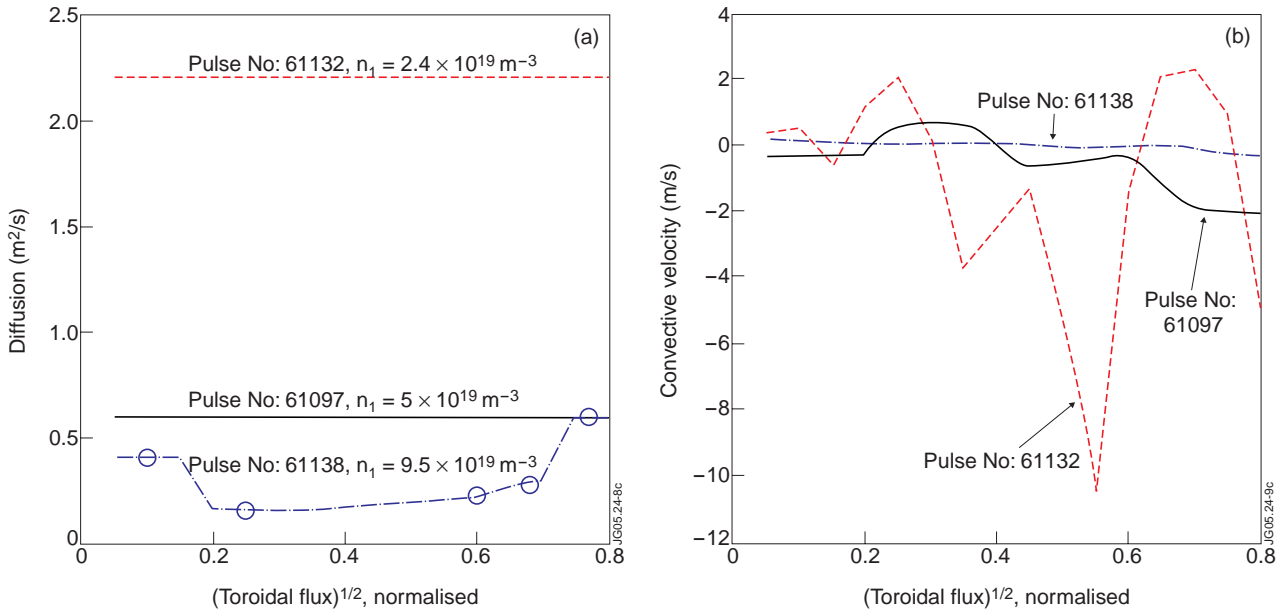


Figure 4: Tritium diffusion (top) and convective velocity (bottom) matching the neutron data as shown in Fig.3. A reasonable fit of the neutron emission is obtained with flat D_T for the low and medium density plasmas while the piece-wise shape of D_T is needed to match the neutron data in high density Pulse No: 61138.

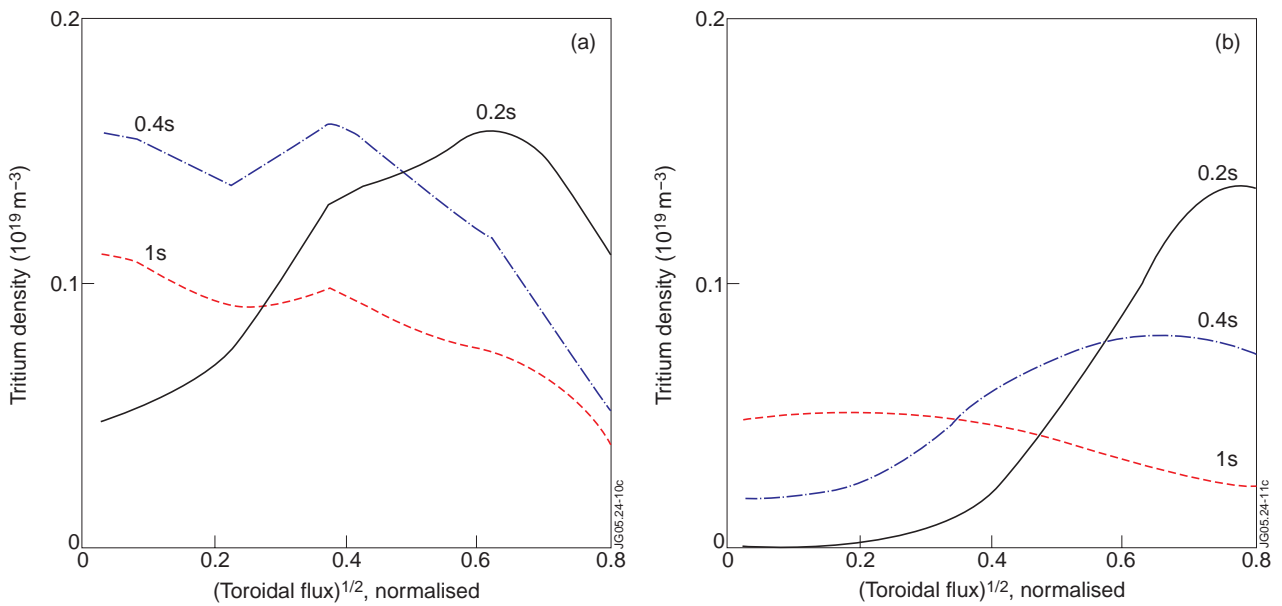


Figure 5: Tritium density profiles for the Pulse Nos: 61097 ($n_1 = 5 \cdot 10^{19} \text{ m}^{-3}$, top) and 61138 ($n_1 = 9.5 \cdot 10^{19} \text{ m}^{-3}$, bottom) calculated with the transport coefficients shown in Fig.4. Time after puff is indicated.

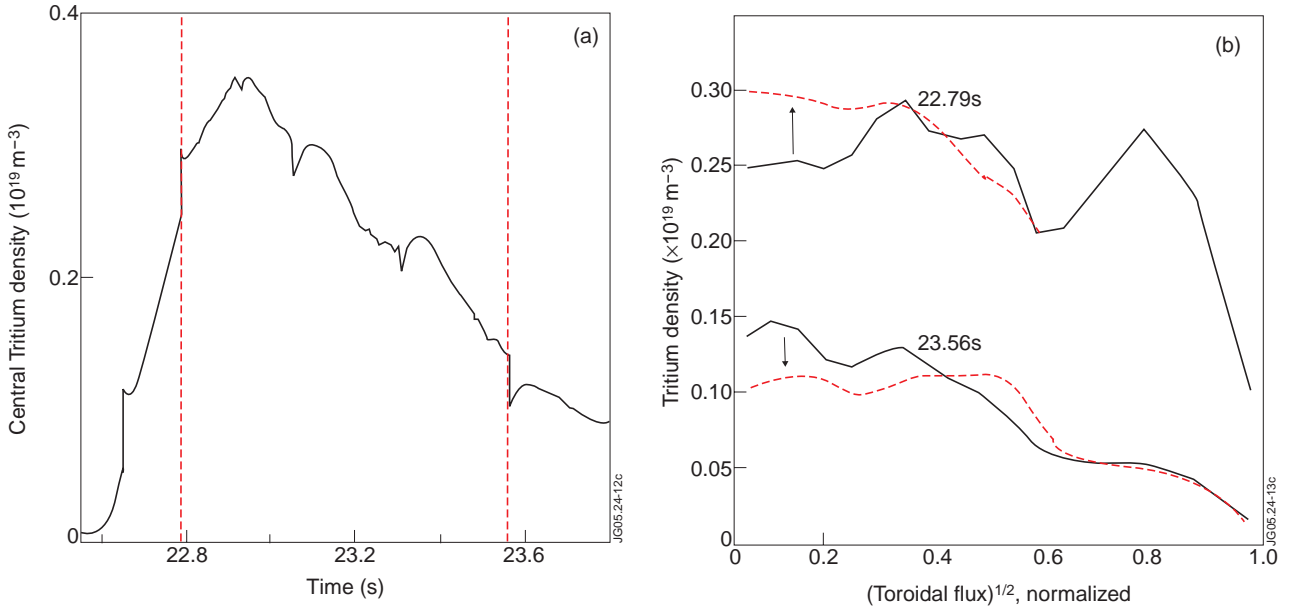


Figure 6: Time evolution of central tritium density (a) and evolution of the tritium density profile during the sawtooth crashes (b) marked by vertical dashed lines in (a) in Pulse No: 61132. The profiles before and after the sawtooth crash are shown by solid and dashed curves correspondingly.

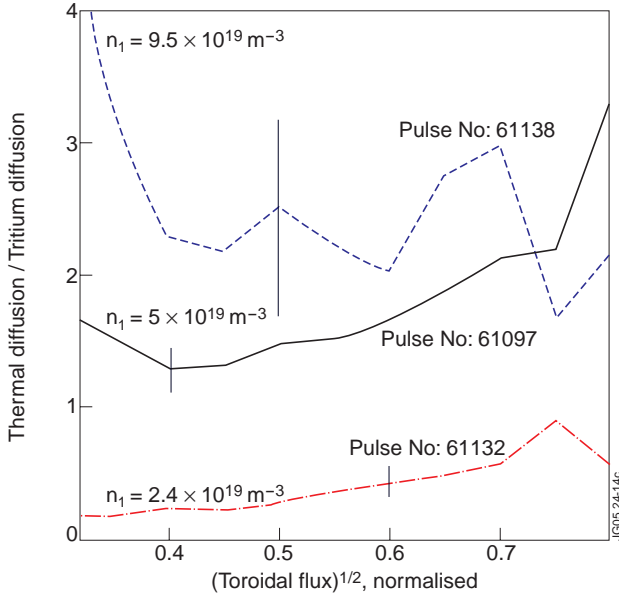


Figure 7: The ratio of thermal effective diffusivity to tritium diffusion coefficient in gradient region. The thermal diffusivity is averaged over 1s during the tritium puff. The error bars for the thermal diffusivity are estimated as a maximum deviation from the averaged value during the time of averaging and divided by the D_T value.

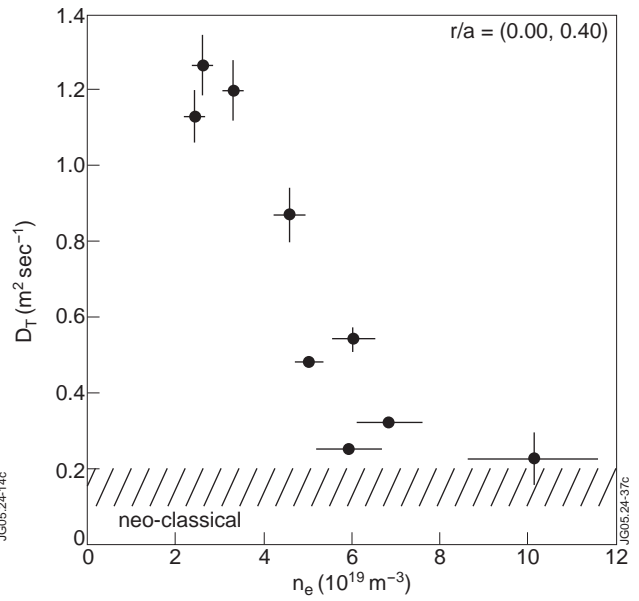


Figure 8: The core tritium diffusion coefficient derived by least-square fit of transport model to experimental data [8, 24] for H-mode plasmas as a function of core plasma density. The error bars for the diffusion coefficient are determined by statistical errors of neutron measurements. The density was averaged over the core region ($r/a < 0.4$) and over the time of the tritium puff and its error bars are determined by the deviation from the averaged value. The range of neoclassical diffusion coefficients estimated for these discharges is indicated.

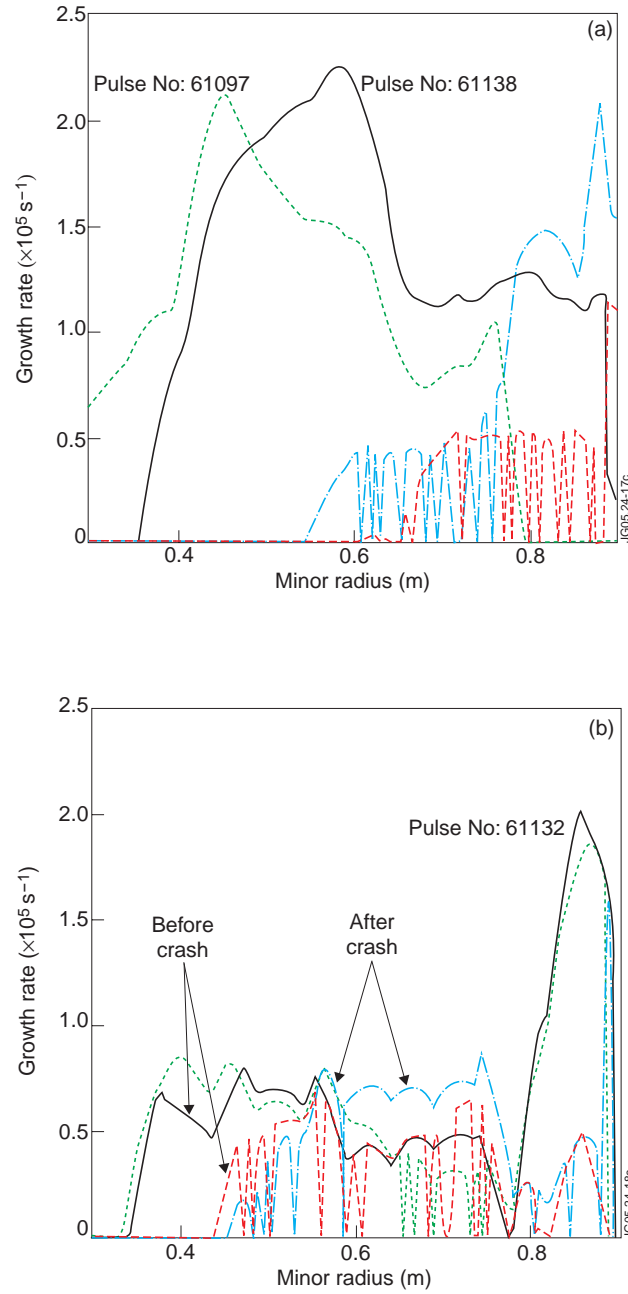


Figure 9: The ITG (solid curves) and TEM (dashed curves) linear growth rates during the tritium puff in Pulse No: 61138 (thin curves) and 61097 (bold curves) (a) and in Pulse No: 61132 (b).

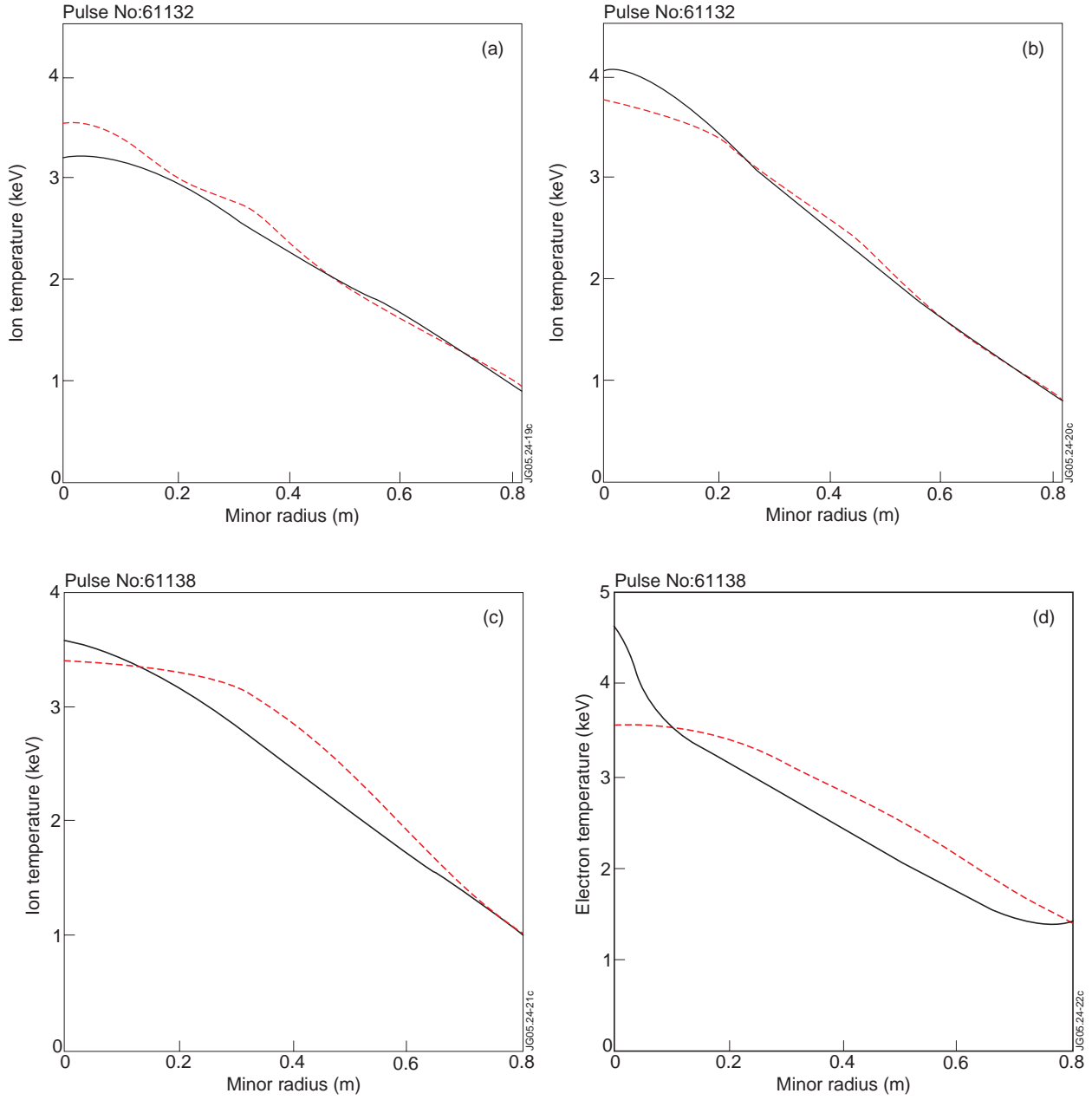


Figure 10: Simulated (solid curves) and experimental (TRANSP fit, dashed curves) ion and electron temperature profiles for Pulse No: 61132 at 22.8s ((a) and (b)) and 61138 at 17.5s ((c) and (d)).

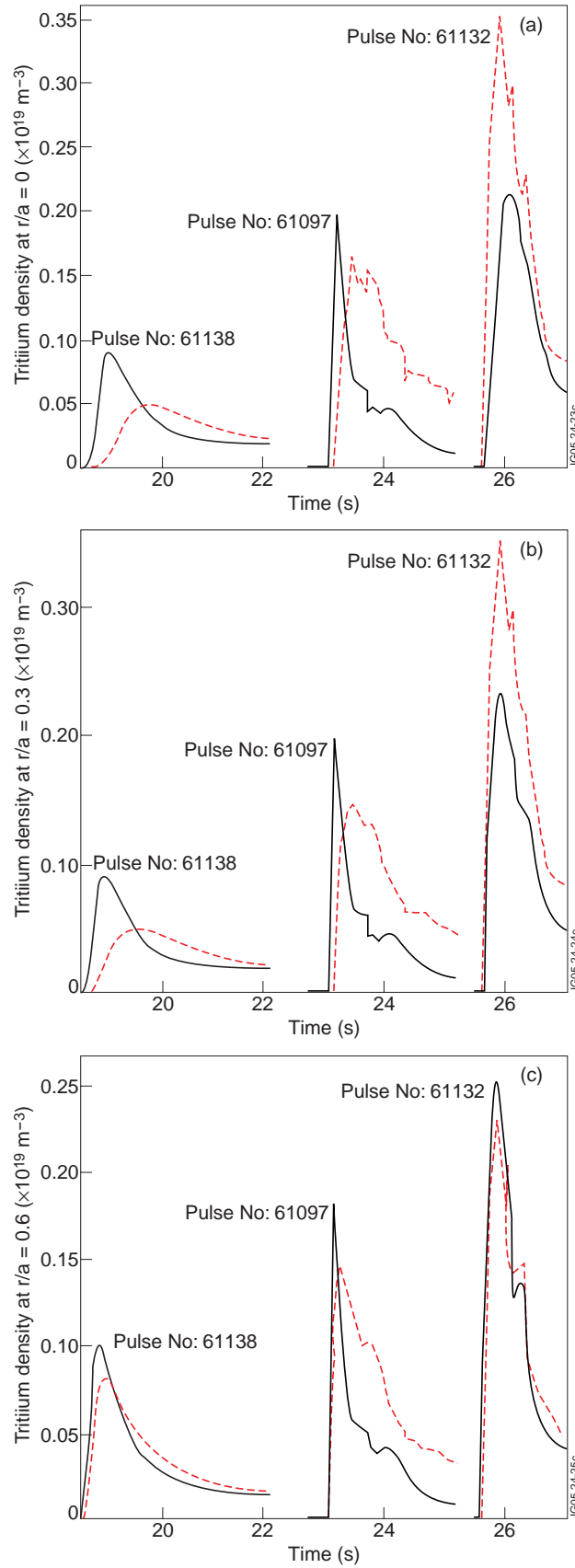


Figure 11: Evolution of tritium density at $r/a = 0$ (a), 0.3 (b) and 0.6 (c) matching the neutron data as shown in Fig.3 (dashed curves) and the density simulated with the MMM model (solid curves). The time shift of 3s is used for Pulse No: 61132 for clarity of display.

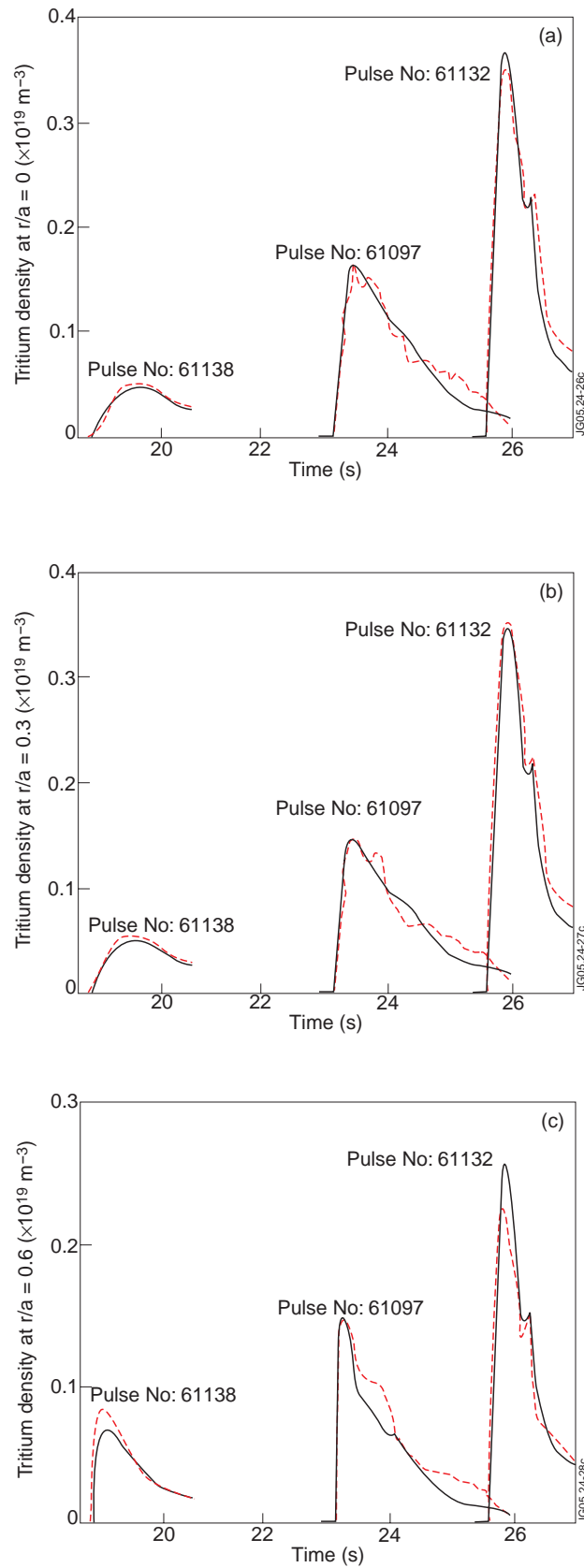


Figure 12: Evolution of tritium density at $r/a = 0$ (a), 0.3 (b) and 0.6 (c) matching the neutron data as shown in Fig.3 (dashed curves) and simulated with the model described by Eq.(1) (solid curves). The time shift of 3s is used for Pulse No: 61132 for clarity of display.

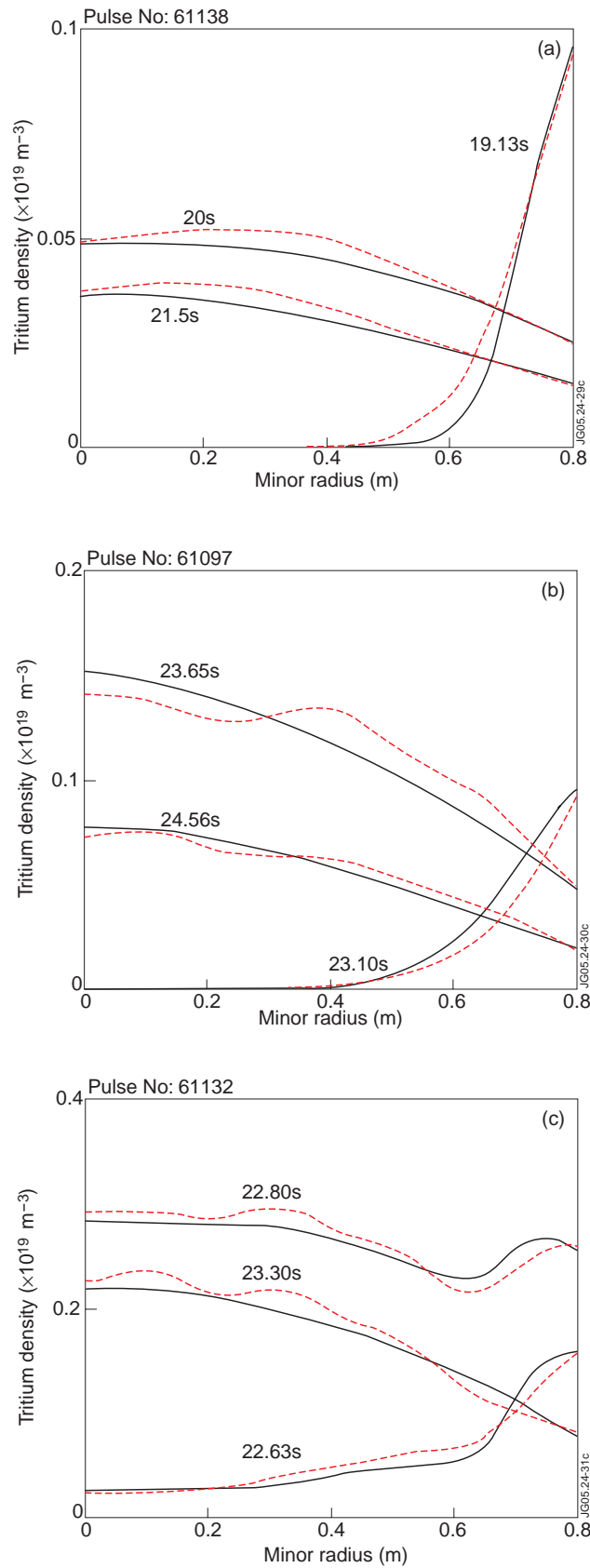


Figure 13: Tritium density profiles obtained in the interpretative analysis (dashed curves) and in predictive modelling shown in Fig.12 (solid curves) during the density rise, peak and decay phases for Pulse Nos: 61138 (a), 61097 (b) and 61132 (c).

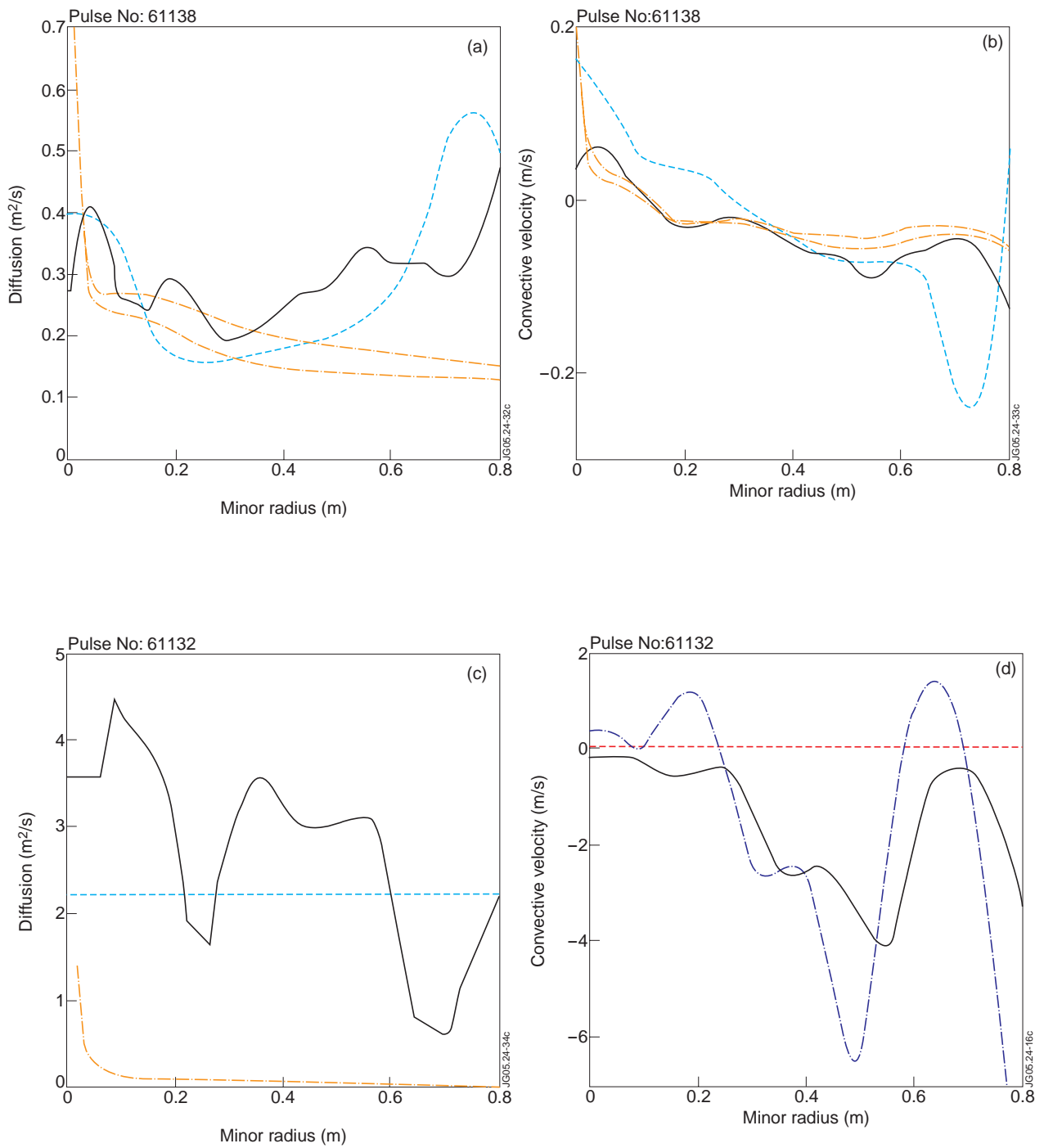


Figure 14: Tritium diffusion and convective velocity calculated with the model of Eq.(1) for Pulse Nos: 61138 ((a) and (b)) and 61132 ((c) and (d)) and used in the simulations shown in Figs.12 and 13 (solid curves). The upper and low limits of neoclassical transport calculated using the error bars of the measurements of electron and ion temperatures, electron density and Z_{eff} are shown by grey dotted curves. The coefficients used in TRANSP simulations (Fig.4) are shown by dashed-dotted curves.